

See discussions, stats, and author profiles for this publication at: <https://www.researchgate.net/publication/261371934>

Variational method for untangling and optimization of spatial meshes

Article in *Journal of Computational and Applied Mathematics* · October 2014

DOI: 10.1016/j.cam.2014.03.006

CITATIONS

3

READS

65

3 authors, including:



[Vladimir A. Garanzha](#)

Russian Academy of Sciences

34 PUBLICATIONS **108** CITATIONS

[SEE PROFILE](#)



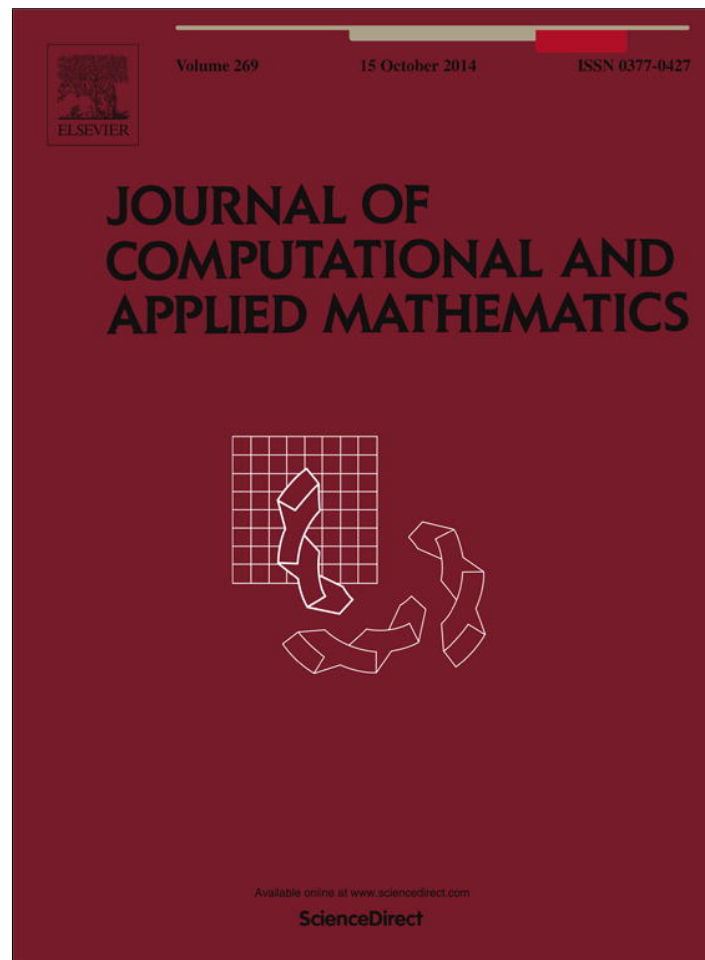
[Sergey Utyuzhnikov](#)

The University of Manchester

137 PUBLICATIONS **716** CITATIONS

[SEE PROFILE](#)

Provided for non-commercial research and education use.
Not for reproduction, distribution or commercial use.



This article appeared in a journal published by Elsevier. The attached copy is furnished to the author for internal non-commercial research and education use, including for instruction at the authors institution and sharing with colleagues.

Other uses, including reproduction and distribution, or selling or licensing copies, or posting to personal, institutional or third party websites are prohibited.

In most cases authors are permitted to post their version of the article (e.g. in Word or Tex form) to their personal website or institutional repository. Authors requiring further information regarding Elsevier's archiving and manuscript policies are encouraged to visit:

<http://www.elsevier.com/authorsrights>



Contents lists available at ScienceDirect

Journal of Computational and Applied Mathematics

journal homepage: www.elsevier.com/locate/cam

Variational method for untangling and optimization of spatial meshes

V.A. Garanzha^{a,b,*}, L.N. Kudryavtseva^{a,b}, S.V. Utyuzhnikov^{b,c}^a Dorodnicyn Computing Center of RAS, Moscow, Vavilova 40, Russia^b Moscow Institute of Physics and Technology, Doldorpuyny, 141700, Russia^c The University of Manchester, School of MACE, Manchester, M13 9PL, UK

ARTICLE INFO

Article history:

Received 4 February 2013

Received in revised form 24 February 2014

Keywords:

Variational mesh generation

Mesh untangling

Barrier functional

Quasi-isometric mapping

Polyconvexity

ABSTRACT

A variational method that can provably construct 3D quasi-isometric mappings between domains of a complex shape is introduced. A local maximum principle for polyconvex mesh element distortion measures is formulated. It allows us to control the invertibility and distortion bounds for non-simplicial elements in the minimization process. A simple and efficient technique for construction of boundary orthogonal meshes suggested in Garanzha (2000) is applied to the construction of hexahedral meshes and thick prismatic mesh layers around complex shapes. The mesh untangling technique, which is a generalization of the penalty method suggested in Garanzha and Kaporin (1999), is verified on a wide set of challenging test problems. Another untangling technique based on theoretical ideas from Ivanenko (1997) is implemented and tested. It provably constructs admissible meshes using a finite number of minimization steps. A minimization technique for the mesh distortion functional is described. The approach is based on the global gradient search technique with preconditioning and domain decomposition for local mesh optimization and untangling. Application areas for explicit and implicit minimization methods are evaluated.

© 2014 Published by Elsevier B.V.

1. Introduction

The aim of mesh optimization is to control shape, size and orientation of mesh elements in order to satisfy mesh quality requirements. The problem of optimization becomes much more difficult if mesh adaptation is also included which implies construction of the mesh which maximizes certain quality and/or efficiency functional of the solution of certain PDE, e.g. the Navier–Stokes equations. In this paper we focus our attention on mesh optimization via node displacement without topological changes. Variational methods proved to be the most robust techniques for optimization of planar, surface and volume meshes [1–14]. The nondegeneracy condition for resulting mesh can be formulated as a set of explicit constraints and resulting variational methods which are generally termed constrained optimization techniques guarantee that mesh be nondegenerate. In the presented approach there is no need to include invertibility conditions as a set of explicit constraints while other types of constraints may appear.

The term “mesh untangling” is generally used when initial guess for the mesh optimization process contains folded and inverted elements or self-overlaps. Hence, a preliminary stage of untangling, which intuitively is very similar to untangling of fisherman net or volleyball net, should be applied. The untangling can be local if just a few elements are folded and one can

* Corresponding author at: Dorodnicyn Computing Center of RAS, Moscow, Vavilova 40, Russia.
E-mail addresses: garan@ccas.ru, numgrid2008@yandex.ru (V.A. Garanzha).

easily extract a relatively small subdomain containing them. The global untangling problem is tightly related to the problem of numerical construction of homeomorphisms between domains with complex shape. Note that one may consider a related problem of least squares matching between domains via deformation in the class of diffeomorphisms. In [15] numerical matching results for 2d and 3d cases were presented. Theoretical foundations of the algorithm can be found at [16]. Untangling is not required in this case.

Several approaches to the untangling problem were developed earlier [5,17–28].

Attempts have been made recently to make finite element approximations suitable for tangled meshes [29]. Analysis is still required to check whether results from [29] are applicable when accurate numerical fluxes are needed or when tangled mesh elements get outside computational domain.

In the beginning of 1990s, Godunov formulated the basic principle of optimal variational meshing such that a mesh should be constructed via a convergent approximation of quasi-isometric mapping. By definition the ratio of the length of any simple curve to the length of its image under quasi-isometric mapping is bounded above by a constant K and bounded below by $1/K$. The mapping should be the unique solution of a variational problem. The variational problem in turn should be constructed using the distortion measures based on principal invariants of the metric tensor of deformation. The discretized variational problem should also have a unique solution. Implementation of these ideas was first presented in [30] using the conformal mapping technique for the problem of constructing parametrization of curvilinear quadrangle. However, in the case of a general domain such a problem has still not been solved even in the 2D case. These ideas inspired a series of papers [31,25,32–34] where the variational principle for construction of multidimensional quasi-isometric mappings was suggested and justified.

In geometrical modeling, the concept of the quasi-isometry is very natural since it provides the rigorous formulation of the intuitive concept of quasi-uniform meshes and deformations with minimal distortion, see review [35].

We describe below a theoretical background for the mesh optimization based on the variational principle for construction of quasi-isometric mappings. The iterative minimization algorithm is also briefly given. The general formulation of variational mesh optimization in implicit domains with slip boundary conditions is provided. Some applications to untangling and optimization of block-structured, hexahedral and prismatic meshes are considered.

2. Variational principle of hyperelasticity in Lagrangian coordinates

The theory of finite hyperelasticity in fact studies the construction of homeomorphisms (elastic deformations) with controlled properties. Application of these ideas to mesh generation is very natural. It was first done in papers by Jacquotte [4,36], see also [17,37]. Let us explain how hyperelasticity principle can be used to construct quasi-isometric mappings.

Let ξ_1, ξ_2, ξ_3 denote the Lagrangian coordinates associated with elastic material, and x_1, x_2, x_3 denote the Eulerian coordinates of a material point. Spatial mapping $x(\xi) : \mathbb{R}^3 \rightarrow \mathbb{R}^3$ defines a stationary elastic deformation. The Jacobian matrix of the mapping $x(\xi)$ is denoted by C , where $c_{ij} = \partial x_i / \partial \xi_j$.

We look for the elastic deformation $x(\xi)$ that minimizes the following stored energy functional

$$F(x) = \int_{\Omega} \Phi(C) d\xi, \tag{1}$$

where $\Phi(C)$ is the elastic potential (internal energy), and domain Ω defines elastic body in the Lagrangian coordinates.

The elastic potential should have the following properties.

(a) Invariance and objectivity: The internal energy should be insensitive to coordinate frame translation and rotation. Hence, $\Phi(UC) = \Phi(C)$, where $U, \det U = 1$ is an orthogonal matrix. If the elastic material is isotropic, the internal energy is invariant with respect to the Lagrangian frame rotation, namely, $\Phi(CV^T) = \Phi(C)$, where $V, \det V = 1$ is an orthogonal matrix as well.

Hence,

$$\Phi(UCV^T) = \Phi(C),$$

where $U^T U = I, \det U = 1, V^T V = I, \det V = 1$ and function $\Phi(C)$ can be expressed as a symmetric function of singular values σ_i of matrix C . Equivalently, this means that $\Phi(C)$ can be represented as a function of the principal invariants of matrix $C^T C$.

(b) Isometry preservation: The absolute minimum of $\Phi(C)$ is attained when $C = U$, where $U^T U = I, \det U = 1$. In fact, the stored energy should reach the minimal value when elastic body is not deformed, i.e. when mapping $x(\xi)$ is isometric.

(c) Linear elasticity limit: In the case of small deformations the hyperelastic material behavior should be described by the linear elasticity equations resulting from Hooke's law. Technically speaking, for the elastic potential the following expansion should be valid

$$\Phi(C) = \Phi(I) + \frac{\lambda}{2} (\text{tr } \mathcal{E})^2 + \mu \text{tr } \mathcal{E}^2 + o(\|\mathcal{E}\|^2),$$

where $\mathcal{E} = \frac{1}{2}(C^T C - I)$ is the Green–Saint-Venant deformation tensor, λ and μ are the Lamé coefficients.

The theorems of existence for solutions of stationary hyperelasticity problems were formulated in the papers by Ball [38,39]. These results are based on the following additional requirements.

- Regularity: elastic deformation is assumed to be the Sobolev mapping;
- Barrier property: $\Phi(C) \rightarrow +\infty$ when $\det C \rightarrow +0$. This property is incompatible with the convexity of function $\Phi(C)$.
- Polyconvexity: function $\Phi(C)$ is called polyconvex if it is the continuous convex function of the minors of matrix C , i.e. there exists continuous convex function $\Phi(C) = \Phi(C, \det C, \text{cof } C)$;
- Penalty for large deformations: function $\Phi(C)$ should satisfy certain growth conditions.

Ball [39] formulated sufficient conditions for elastic deformations to be homeomorphisms which are not smooth but regular enough for deformation as a function of Lagrangian coordinates to belong to a certain Sobolev space. Omitting technical details, one can formulate the theorems of existence as follows. Suppose that there exists at least one Sobolev homeomorphism which belongs to a certain admissible set and provides finite value for the stored energy functional. Then, the minimizer of the hyperelasticity problem exists and is the Sobolev homeomorphism as well. The proof technique is based on the so-called direct method via the analysis of minimizing sequences. For direct method existence of the global minimizing sequence is established. However the existence proof is not constructive hence in practice local minimizing sequences are constructed.

A practical conclusion from the theoretical results given above is that construction of an admissible Sobolev homeomorphism is obviously related to the mesh untangling while the construction of a minimizing sequence is related to mesh optimization.

Ball proved [38] that every polyconvex function $\Phi(C)$ is rank one convex, namely

$$\begin{aligned} \Phi(\lambda C_1 + (1 - \lambda)C_2) &\leq \lambda\Phi(C_1) + (1 - \lambda)\Phi(C_2), \\ \text{rank}(C_1 - C_2) &= 1, \quad 0 \leq \lambda \leq 1. \end{aligned} \tag{2}$$

If in addition function $\Phi(C)$ is twice continuously differentiable, then rank one convexity is equivalent to the Hadamard–Legendre condition

$$\sum_{i,j,k,p=1}^d \frac{\partial^2 \Phi}{\partial c_{ik} \partial c_{jp}} p_i p_j r_k r_p \geq 0, \tag{3}$$

where $p, r \in \mathbb{R}^3$ are arbitrary vectors. This inequality is also called the ellipticity condition for the Euler–Lagrange equations of the functional (1).

A simple transformation can be applied to the elastic potential to make the singular mappings inadmissible. Let $W(C)$ denote the elastic potential. For $1 < \alpha < +\infty$ consider the following transformation:

$$W_\alpha(C) = \begin{cases} \frac{1}{\alpha} \frac{(\alpha - 1)^2 W(I) W(C)}{\alpha W(I) - W(C)} & \text{when } W(C) < \alpha W(I) \\ +\infty & \text{when } W(C) \geq \alpha W(I). \end{cases} \tag{4}$$

Potential $W_\alpha(C)$ is finite only if

$$W(C) < \alpha W(I). \tag{5}$$

The Lamé coefficients λ and μ of the potentials $W(C)$ and $W_\alpha(C)$ coincide. Parameter α is used to control the upper bound of deformation (quasi-isometry constant).

The general properties of the elastic potential can be understood better when the theorems of existence for the variational problem are formulated. Let us note that the formulated requirements differ from those formulated in Ball’s theorems.

Let Ω be a bounded Lipschitz domain in \mathbb{R}^3 . Consider the stored energy functional $F_\alpha(x)$ which can be written as

$$F_\alpha(x) = \int_{\Omega} W_\alpha(\nabla_\xi x) \, d\xi, \tag{6}$$

where function $W_\alpha(C)$ is defined in (4), and $C = \nabla_\xi x$ is the Jacobian matrix of the mapping $x(\xi)$.

Let us define the set of admissible deformations \mathcal{A}_α via

$$\mathcal{A}_\alpha = \{y \in \mathbb{W}_p^1(\Omega), p > 3, W(\nabla_\xi y) < \alpha W(I) \text{ almost everywhere in } \Omega\} \tag{7}$$

where \mathbb{W}_p^1 is the standard notation for the Sobolev space with the norm defined by

$$\|y\|_{\mathbb{W}_p^1} = \left(\int_{\Omega} \sum_i (|y_i|^p + |\nabla_\xi y_i|^p) \, d\xi \right)^{\frac{1}{p}}.$$

It is assumed that the function $W(C)$ has the following properties:

- (P1) $W(C) : \mathbb{R}^{3 \times 3} \rightarrow \bar{\mathbb{R}}$ is a polyconvex function;
- (P2) $W(C) \geq W(U) = W(I) > 0$, for any U such that $U^T U = 1, \det U = 1$;

(P3) there exist continuous monotone increasing locally bounded functions $\phi_1(\alpha)$, $\phi_2(\alpha)$ such that $\phi_i(1) = 1$, $\phi_i(+\infty) = +\infty$, and from inequality $W(C) < \alpha W(I)$ it follows that

$$\det C > \frac{1}{\phi_1(\alpha)}, \quad \frac{1}{\phi_2(\alpha)} < \sigma_i(C) < \phi_2(\alpha)$$

(P4) there exists continuous monotone increasing locally bounded function $\phi_3(\alpha)$ such that if $\det C > 0$ and C satisfies inequality $\frac{1}{\phi_3(\alpha)} < \sigma_i(C) < \phi_3(\alpha)$, then $W(C) < \alpha W(I)$.

Here, $\sigma_i(C)$ denotes the i th singular value of the matrix C .

Theorem 2.1. Suppose that function $W(C)$ satisfies conditions (P1)–(P4). Let Ω , $\Omega_1 \subset \mathbb{R}^3$ be bounded Lipschitz domains such that there exists a quasi-isometric mapping $y_0(\xi) : \bar{\Omega} \rightarrow \bar{\Omega}_1$, $y_0 \in \mathcal{A}_{\alpha_0}$ and $F_{\alpha_0}(y_0) < +\infty$ for certain $1 < \alpha_0 < +\infty$.

Then, there exists $x^*(\xi) \in \mathcal{A}_{\alpha_0}$ such that

$$F_{\alpha_0}(x^*) = \inf_{y \in \mathcal{A}_{\alpha_0}, y|_{\partial\Omega} = y_0|_{\partial\Omega}} F_{\alpha_0}(y) \tag{8}$$

and $x^*(\xi) : \bar{\Omega} \rightarrow \bar{\Omega}_1$ is a quasi-isometric mapping.

The proof of the theorem can be found in [34].

For mesh generation in [31] it was suggested to use the polyconvex elastic potential represented by a sum of shape distortion and volumetric distortion terms:

$$W(C) = (1 - \theta) \frac{\left(\frac{1}{3}\text{tr}(C^T C)\right)^{3/2}}{\det C} + \frac{1}{2}\theta \left(\frac{1}{\det C} + \det C\right). \tag{9}$$

Here, parameter θ plays the role of the volumetric modulus, while $1 - \theta$ is the shear modulus. The Lamé coefficients do not have geometrical meaning so it is not advisable to prescribe them directly. They can be expressed in terms of shear modulus and volumetric modulus.

Functional (6) and (9) essentially measures the deviation of mapping from isometry. It can be used to construct quasi-uniform meshes. In fact, formula (9) generates a family of mesh generation functionals.

Incompressible deformations are not included into the above analysis. However almost incompressible deformations can be simulated setting $\theta \approx 1$. Experience of authors shows that construction of almost incompressible finite deformations is quite tricky in a sense that it may create multiple solutions relatively easily. This topic is beyond the scope of the paper.

A simple variant of mesh optimization and smoothing can be obtained using

$$W_s(C) = \frac{\left(\frac{1}{3}\text{tr}(C^T C)\right)^{3/2}}{\det C}.$$

The resulting functional is used for many years in the theory of quasi-conformal mappings. It is scale invariant and can be applied only for mesh element shape optimization. Note that in many cases it can lead to appearance of very large or small elements. A family of scale invariant distortion measures is presented in [6]. One can also use another shape distortion measure (see, e.g. [40,10,26])

$$\tilde{W}_s(C) = \frac{\frac{1}{3}\text{tr}(C^T C)}{\det C^{2/3}}.$$

This scale invariant distortion measure is polyconvex as well. The properties of these two distortion measures are similar, however, $W_s(C)$ is more sensitive to distortion. If these measures are bounded, then the singular condition number of the matrix C (namely, the ratio of any singular values) is bounded. Unfortunately existence theorems cannot be applied for this class of distortion functionals due to the lack of proper growth conditions.

When the control over mesh size is desirable, one can use a balanced distortion measure (9)

$$W(C) = \frac{\phi_\theta(C)}{\det C}, \quad \phi_\theta(C) = (1 - \theta) \left(\frac{1}{3}\text{tr}(C^T C)\right)^{3/2} + \frac{1}{2}\theta(1 + \det C^2). \tag{10}$$

Numerical experiments in [31,24] suggested that $\theta = 4/5$ should be used for balanced distortion measure. Larger values of θ make the hyperelastic material behave close to the incompressible one and may potentially result in instabilities in the case of large deformations.

The most complex distortion measure among considered is the quasi-isometric distortion measure [31] which is constructed as a combination of (4) and (9), and can be written as follows:

$$W_t(C) = (1 - t) \frac{\phi_\theta(C)}{\det C - t\phi_\theta(C)}. \tag{11}$$

Here, parameter $\alpha = 1/t$ plays the role of the global upper bound of distortion. The particular choice of the distortion measure depends on the application. For the mesh smoothing problems a simple shape distortion is a good choice. For problems

such as construction of global mappings, flattening of 2D and 3D manifolds and many others, a balanced distortion measure can be used, while application of quasi-isometric distortion measure being critical for the problems where control over worst elements is crucial. For example, in [41,42], max-norm optimization of element quality is used for improvement of the worst mesh elements in 3D mesh. Here, instead of applying the max-norm optimization strategy, one has to solve the sequence of variational problems with the distortion measure (11) using the continuation technique that maximizes the parameter t .

In practice, one can control the spatial distribution of distortion measure without actual contraction of the feasible set. It is possible to introduce a weight function in the Lagrangian coordinates which takes large values in critical regions and is close to unity elsewhere. The weighted distortion measure looks as follows:

$$W_w(C) = w(\xi) \frac{\phi_\theta(C)}{\det C}. \tag{12}$$

In the process of minimization, elements with a larger weight tend to have a smaller value of distortion function $W(C)$. Hence, their shapes and sizes are very close to the target ones. This simple approach proved to be very efficient for mesh orthogonalization near the boundary [43,31]. A proper choice of the weight allows us to satisfy the no-slip boundary conditions and to approximate boundary orthogonality conditions and prescribed mesh size in the normal direction very accurately. Prescribed intersection angle boundary conditions can be approximated as well.

Theoretical arguments suggest that in order to eliminate the local singularities of the distortion function the weight distribution should be singular. However, this singularity is only reached in the limit of mesh refinement and for any given finite mesh weight distribution is bounded.

Let $G_\xi(\xi)$ and $G_x(x)$ denote the metric tensors defining linear elements and length of curves in Lagrangian and Eulerian coordinates in the domains Ω_ξ and Ω_x , respectively. Then, $x(\xi)$ is the mapping between metric manifolds M_ξ and M_x . The distortion functional for this mapping can be written as

$$F_\alpha(x) = \int_{\Omega_\xi} W_\alpha(Q \nabla_\xi x H^{-1}) \det H d \xi, \tag{13}$$

where

$$H^T H = G_\xi, \det H > 0, \quad Q^T Q = G_x, \det Q > 0$$

are arbitrary matrix factorizations of metric tensors G_ξ and G_x . If certain quasi-isometric parameterizations $\eta(\xi)$ and $y(x)$ of manifolds M_ξ and M_x already exist, then one can simply use the functional suggested in (6) for mapping $y(\eta)$ and apply the chain rule to obtain the variational formulation for mapping $x(\xi)$ which coincides with (13) provided that

$$H = \nabla_\xi \eta, \quad Q = \nabla_x y.$$

The functional (13) is invariant with respect to the coordinate transformation in Lagrangian and Eulerian coordinates [32]. Hence, the composition of mappings $y \circ x^* \circ \eta^{-1}$ does not depend on the initial parameterizations $\eta(\xi)$ and $y(x)$, where $x^*(\xi)$ is mapping minimizing the functional (13). Functional (13) only depends on the principal invariants of matrix $C^T G_x C G_\xi^{-1}$. The existence theorem can be generalized for this case under additional regularity conditions on function $G_x(x)$.

In [21] it was suggested to approximate barrier functional by the penalty functional thus relaxing condition $\det \nabla_\xi x > 0$ for the set of admissible mappings. The idea is to replace $\det C$ in the denominator of elastic potential by the function

$$\chi_\varepsilon(\det C) = \frac{1}{2}(\det C + \sqrt{\varepsilon^2 + \det C^2}). \tag{14}$$

Thus functional (13) is approximated by

$$\Phi_\varepsilon(x) = \int_{\Omega_\xi} P_\varepsilon(Q \nabla_\xi x H^{-1}) \det H d \xi, \tag{15}$$

where penalty potential $P_\varepsilon(C)$ is defined as follows

$$P_\varepsilon(C) = \frac{\phi_\theta(C)}{\chi_\varepsilon(\det C)}, \tag{16}$$

where $\phi_\theta(C)$ is defined in (10). Note that penalty function (16) generally is not polyconvex and violation of polyconvexity is related to values of $|\det C|$ comparable to ε . One can use functional (15), (16) in order to construct admissible mapping for barrier distortion functional which is explained in the section devoted to iterative solver.

Another way to approximate barrier functional is to extend the set of admissible mappings using barrier elastic potential with a wider admissible set

$$\Psi_\varepsilon(x) = \int_{\Omega_\xi} P_\varepsilon(Q \nabla_\xi x H^{-1}) \det H d \xi, \quad B_\varepsilon(C) = \frac{\phi_\theta(C)}{\det C + \varepsilon}. \tag{17}$$

Note that function $B_\varepsilon(C)$ is polyconvex.

One can use composition of mappings in order to control the local properties of mapping, e.g. to adapt a mesh to the surface curvature. The curvature-sensitive adaptation is very important for resolution of geometrical features and quality meshing of complex-shaped surfaces and solids. In most practical cases, a surface is defined by nonsmooth and noisy data which makes analytical computation of a curvature unfeasible. The curvature sensitive adaptation should be stable with respect to noisy data and provide controllable mesh condensation near sharp edges. Highly skewed elements should not be present.

Consider a parametric surface S in \mathbb{R}^3 defined by the function

$y_1(x_1, x_2), y_2(x_1, x_2), y_3(x_1, x_2)$. The Laplace–Beltrami operator is defined as

$$\Delta_B = \frac{1}{J} \left(\frac{\partial}{\partial x_1} \frac{g_{22}}{J} \frac{\partial}{\partial x_1} - \frac{\partial}{\partial x_1} \frac{g_{12}}{J} \frac{\partial}{\partial x_2} - \frac{\partial}{\partial x_2} \frac{g_{12}}{J} \frac{\partial}{\partial x_1} + \frac{\partial}{\partial x_2} \frac{g_{11}}{J} \frac{\partial}{\partial x_2} \right), \quad (18)$$

where $g_{ij} = \sum_k \frac{\partial y_k}{\partial x_i} \frac{\partial y_k}{\partial x_j}$ are the entries of the first fundamental form G of $S, J = \det G^{\frac{1}{2}}$.

Since

$$\Delta_B y = \nu H, \quad (19)$$

where ν is the unit normal to the surface, and H is the mean curvature, one can use the discrete Laplace–Beltrami operator to calculate the discrete mean curvature.

A special finite volume technique is used to discretize the Laplace–Beltrami operator, which provides second order accurate “fluxes” through dual edges on highly nonuniform almost orthogonal meshes and remains stable on nonconvex quadrilaterals.

Let $G_\xi(\xi)$ and $G_x(x)$ be the metric tensors defining the metrics in Lagrangian and Eulerian coordinates in domains $V_\xi \subset \mathbb{R}^2$ and $V_x \subset \mathbb{R}^2$, respectively. The curvature sensitive 2D distortion functional for optimization of surface meshes can be written as

$$F_\alpha(x) = \int_{V_\xi} W_\alpha(Q \nabla_\xi x P^{-1}) \det P d\xi, \quad (20)$$

where

$$P^T P = G_\xi, \det P > 0, \quad Q^T Q = G_x,$$

are some factorizations of 2×2 matrices.

The metric tensor $G_x(x)$ is given by

$$G_x(x) = (1 + c|H(x)|)I,$$

where $H(x)$ is the mean curvature, c is a constant weight. Distortion function $W_\alpha(C)$ is based on the following 2D elastic potential

$$W(C) = (1 - \theta) \frac{\frac{1}{2} \text{tr}(C^T C)}{\det C} + \frac{1}{2} \theta \left(\frac{1}{\det C} + \det C \right).$$

The case when there is no explicit representation for surface S should be considered as well. Then $S \subset \partial\Omega$, where $\Omega \subset \mathbb{R}^3$ is a bounded domain, $\partial\Omega$ is defined as zero isosurface of certain piecewise regular Lipschitz function $u(y)$. It is assumed that $u(y) < 0$ at interior points of the domain Ω , $u(y) > 0$ in the complement of the domain, its derivatives along a certain nondegenerate vector field transversal to $\partial\Omega$ exist and do not vanish in a certain finite layer R near $\partial\Omega$. In fact, we assume that the behavior of the implicit function u qualitatively resembles the behavior of the signed distance function.

Then, in the neighborhood of each point $p \in S$ one can find the coordinate frame such that S locally is the graph of Lipschitz continuous height function $y(x)$ which essentially provides surface parametrization. Thus the iterative method for surface mesh optimization can be applied.

3. Discretization of distortion measures and minimization technique

Consider mapping $x(\xi)$ from parametric domain $\Omega_\xi \subset \mathbb{R}^3$ onto computational domain $\Omega_x \subset \mathbb{R}^3$. Suppose that domain Ω_ξ admits normal tiling by canonical elements K_k .

The distortion measure of the mapping $x(\xi)$ can be approximated by the following semidiscrete functional

$$F_\alpha(x_h(\xi)) = \sum_{K_k} \int_{K_k} W_\alpha(\nabla x_h(\xi)) d\xi,$$

where $x_h(\xi)$ is certain continuous piecewise-smooth mapping.

If all canonical elements K_k are simplices, then the mapping $x_h(\xi)$ on each element can be chosen to be affine, and the local Jacobian matrix is constant. Hence,

$$F_\alpha(x_h(\xi)) = \sum_k W_\alpha(\nabla x_h(\xi))|_{K_k} \text{vol}(K_k) = F_\alpha^h(x_h(\xi)),$$

where $F_\alpha^h(x_h(\xi))$ denotes fully discrete functional.

If the local mapping is not affine, the quadrature rules should be used to approximate the contribution from each element. When $G_\xi = I$ and $G_x = I$ then for a certain class of continuous piecewise-polynomial mappings quadrature rules were suggested in paper [25], which in the case of polyconvex function $W_\alpha(C)$ guarantee that

$$F_\alpha(x_h(\xi)) \leq F_\alpha^h(x_h(\xi)). \tag{21}$$

This property is very important since it guarantees that once an initial guess is admissible mapping, namely, it is a quasi-isometric mapping satisfying given constraints and boundary conditions, then in the process of minimization the discrete solution remains admissible.

The geometric quadrature rules are based on the following maximum principle for polyconvex distortion measure, which is a generalization of the result from [25]. Outline of the proof is essentially the same as in [25], but formulation of the theorem is refined.

Theorem 3.1. *Let C_1, \dots, C_m be a set of $d \times d$ matrices, function $f(C)$ is polyconvex, and $U \subset \mathbb{R}^d$ is a convex domain. Assume that the Jacobian matrix of smooth mapping $x(\xi) : \bar{U} \rightarrow \mathbb{R}^d$ is defined by equality*

$$\nabla_\xi x(\xi) = C = \sum_{j=1}^m C_j \Lambda_j(\xi), \quad \sum_{j=1}^k \Lambda_j = I, \quad \Lambda_j \geq 0, \tag{22}$$

where $\Lambda_j(\xi) \in C(\bar{U})$ are diagonal $d \times d$ matrices.

Let $\tilde{C}_\nu, \nu = 1, \dots, m^d$ denote “compound” $d \times d$ matrix, with k th column chosen as k th column of any basis matrix C_i . Suppose that inequality $f(\tilde{C}_\nu) \leq c_0, c_0 > 0$ holds for all values of ν . Then, (a) $f(C) \leq c_0$; (b) one can find the set of coefficients $a_\nu(\xi) \geq 0, \sum_{\nu=1}^{m^d} a_\nu = 1$ such that

$$C(\xi) = \sum_{\nu=1}^{m^d} a_\nu(\xi) \tilde{C}_\nu, \quad f(\nabla_\xi x) \leq \sum_{\nu=1}^{m^d} a_\nu(\xi) f(\tilde{C}_\nu). \tag{23}$$

Now assume that U is a canonical mesh element in the parametric space which could be a regular or semi-regular polyhedron. Let us assume that the Jacobian matrix of mapping $x^h(\xi) : \bar{U} \rightarrow \mathbb{R}^d$ is defined by $\nabla_\xi x^h = \sum_{i=1}^m C_i \Lambda_i(\xi)$.

To construct a discrete distortion measure of the image of element U , one can use the following quadrature rule:

$$\int_U f(\nabla_\xi x^h) d\xi \approx \sum_{q=1}^{N_q} \beta_q f(\tilde{C}_q) \text{vol}(U), \quad \beta_q = \frac{1}{\text{vol}(U)} \int_U a_q d\xi, \quad N_q = m^d, \tag{24}$$

where a_q is the set of coefficients from Theorem 3.1. The inequality (21) is a direct consequence of (23). Summing up contributions from all mesh elements, one can compute fully discrete functional $F_\alpha^h(x_h(\xi))$.

The resulting geometric quadratures are exact for constant functions and for the determinant of the Jacobian matrix. If the parametric domain U is centrally symmetric in the sense that the integral of any linear function of ξ taking zero value at its center is zero then the quadratures are exact on linear functions.

The maximum principle can be applied to the polyconvex distortion measures for bilinear quadrangles, trilinear hexahedra, pyramids and prisms, quadratic triangular and tetrahedral isoparametric elements and to arbitrary order Bernstein-Bezier polynomials.

In [44], a sufficient condition was derived for invertibility of the Bernstein-Bezier polynomial mappings.

In 1D the Bernstein-Bezier polynomial of the order of p defined on interval $0 \leq \xi \leq 1$ can be written as follows (e.g. [45]):

$$u(\xi) = \sum_{i=0}^p u_i \xi^i (1 - \xi)^{p-i} \frac{p!}{i!(p-i)!}. \tag{25}$$

Equality (25) is nothing else but the convex combination of $p + 1$ control points u_i

$$\sum_{i=0}^p \xi^i (1 - \xi)^{p-i} \frac{p!}{i!(p-i)!} = (\xi + (1 - \xi))^p = 1.$$

The first derivative of $u(\xi)$ is given by

$$\frac{\partial u}{\partial \xi} = \sum_{i=0}^{p-1} p(u_{i+1} - u_i) \xi^i (1 - \xi)^{p-i-1} \frac{(p-1)!}{i!(p-i-1)!}. \tag{26}$$

Since

$$\sum_{i=0}^{p-1} \xi^i (1 - \xi)^{p-i-1} \frac{(p-1)!}{i!(p-i-1)!} = (\xi + (1 - \xi))^{p-1} = 1,$$

one obtains that the first derivative is a convex combination of p differences $p(u_{i+1} - u_i)$.

To construct the polynomial mapping of multidimensional cube, one can use the tensor product of the 1D Bernstein-Bezier polynomials. Below we consider in the 3D case the following mapping of the unit cube $x(\xi) : \bar{U} \rightarrow \bar{D}$, where $U = \{\xi : 0 < \xi_i < 1\}$ and D is a curvilinear hexahedron. Denote the control points of the spline by x_{ijk} , $i, j, k \in \{0, \dots, p\}$.

$$x(\xi) = \sum_{i,j,k=0}^p x_{ijk} \xi_1^i (1 - \xi_1)^{p-i} \xi_2^j (1 - \xi_2)^{p-j} \xi_3^k (1 - \xi_3)^{p-k} \cdot \frac{p!p!p!}{i!(p-i)!j!(p-j)!k!(p-k)!} \quad (27)$$

The columns c_i of the Jacobian matrix $C = \nabla_{\xi} x$ of polynomial mapping (27) can be written as follows:

$$\begin{aligned} c_1 &= \sum_{i=0}^{p-1} \sum_{j,k=0}^p p(x_{i+1jk} - x_{ijk}) \xi_1^i (1 - \xi_1)^{p-i-1} \\ &\quad \times \xi_2^j (1 - \xi_2)^{p-j} \xi_3^k (1 - \xi_3)^{p-k} \frac{(p-1)!p!p!}{i!(p-i-1)!j!(p-j)!k!(p-k)!} \\ c_2 &= \sum_{j=0}^{p-1} \sum_{i,k=0}^p p(x_{ij+1k} - x_{ijk}) \xi_2^j (1 - \xi_2)^{p-j-1} \\ &\quad \times \xi_1^i (1 - \xi_1)^{p-i} \xi_3^k (1 - \xi_3)^{p-k} \frac{(p-1)!p!p!}{j!(p-j-1)!i!(p-i)!k!(p-k)!} \\ c_3 &= \sum_{k=0}^{p-1} \sum_{i,j=0}^p p(x_{ijk+1} - x_{ijk}) \xi_3^k (1 - \xi_3)^{p-k-1} \\ &\quad \times \xi_1^i (1 - \xi_1)^{p-i} \xi_2^j (1 - \xi_2)^{p-j} \frac{(p-1)!p!p!}{k!(p-k-1)!i!(p-i)!j!(p-j)!} \end{aligned} \quad (28)$$

Hence, the Jacobian matrix admits representation (22)

$$\nabla_{\xi} x = C(\xi) = \sum_{k=1}^m C_k A_k(\xi), \quad A_k(\xi) \geq 0, \quad \sum_{k=1}^m A_k(\xi) = 1,$$

where $A_k(\xi)$ are diagonal matrices, C_k are constant matrices and value m in the 3-dimensional case is equal to $p(p+1)^2$. Hence, the maximum principle for polyconvex distortion measures holds.

When $p = 1$, D is a hexahedron with straight edges. Mapping (27) is just a trilinear mapping

$$x(\xi_1, \xi_2, \xi_3) = \sum_{i,j,k=0}^1 (1 - \xi_1)^{1-i} \xi_1^i (1 - \xi_2)^{1-j} \xi_2^j (1 - \xi_3)^{1-k} \xi_3^k x_{ijk}, \quad (29)$$

$m = 4$ and total number of quadrature “nodes” is equal to $4^3 = 64$.

In practice, simplified quadrature rules are frequently used that can be understood as simplicial approximations of non-simplicial elements. In this case, estimate (21) cannot be rigorously derived but numerical experiments show quite favorable results.

The unknowns of the discretized variational problem are vertices of the mesh in the computational domain. Denote by $z_k \in \mathbb{R}^3$, $k = 1, \dots, n_v$ the vector of k th vertex coordinates, and $Z = (z_1 z_2 \dots z_{n_v})$ is the $3 \times n_v$ matrix of unknowns. Hence the solution of the discrete variation problem with functional $F_{\alpha}^h(x_h(\xi))$ is reduced to minimization of the function $F(Z)$.

4. Iterative minimization scheme

The stationarity condition at the k th internal vertex of the mesh is simply written as $\frac{\partial F}{\partial z_k} = 0$.

For an implicit domain Ω , the slip boundary conditions should be included into the minimization process. Let us assume that vector $\nabla u(z_k)$ be defined. Otherwise, in order to obtain an approximate value of the gradient, one can use the tangent cone at a point that is always defined. Note that, in practice, this approximate value is computed using finite differences. Let us use notation $L_k = (I - \nabla u \nabla u^T / |\nabla u|^2)|_{z_k} \in \mathbb{R}^{3 \times 3}$ if z_k is a vertex on the slip boundary. Multiplication by matrix L_k eliminates the component normal to the local boundary tangent plane. For all other points we set $L_k = I$.

Then the stationarity condition for the function $F(Z)$ at the sliding boundary vertex z_k can be re-written as

$$L_k \frac{\partial F}{\partial z_k} = 0 \quad (30)$$

$$u(z_k) = 0. \quad (31)$$

Let δz_k denote a displacement at the point z_k . Linearizing Eq. (30), one can obtain

$$\delta z_k^T \nabla u(z_k) + u(z_k) = 0.$$

Thus, when $u(z_k) = 0$, displacement δz_k should lie in the tangent plane.

Let us denote by V the operator which projects a point onto $\partial\Omega$ along approximate gradient curves of function $u(x)$.

The gradient R of the function $F(z_1, \dots, z_{n_v})$ is obtained from 3D vectors $r_k = \frac{\partial F}{\partial z_k}$. The Hessian matrix H of F is constructed from 3×3 blocks $H_{ij} = \frac{\partial^2 F}{\partial z_i \partial z_j}$, where matrix H_{ij} is placed on the intersection of the i th block row with j th block column.

Function F is not convex hence matrix H generally is not positive definite. However, it follows from the Hadamard–Legendre inequality (3) that H_{ii} are positive definite matrices. For the proof it suffices to consider variation of F with respect to displacement of a single node. This displacement has rank one in a sense that gradient of resulting deformation at internal points of elements adjacent to this vertex can be represented as the gradient of initial deformation plus rank one matrix. Function F is convex with respect to rank one displacements. Another type of rank one displacement is displacement of all mesh vertices in the same direction with different amplitudes. It means that one can symmetrically reorder matrix H into $9 n_v \times n_v$ blocks such that diagonal blocks are positive definite matrices which correspond to finite element approximations of scalar elliptic operators.

Using the notations given above, one can formulate the following iterative scheme which can be considered as the projected Newton–Raphson method:

$$\sum_{j=1}^{n_v} L_i^T H_{ij} L_j \delta z_j + L_i^T r_i(Z^l) = 0 \tag{32}$$

$$z_k^{l+1} = V(z_k^l + \tau_l L_k \delta z_k), \quad k = 1, \dots, n_v. \tag{33}$$

Parameter τ_l can be found using an approximate solution to the following line search problem

$$\tau_l = \arg \min_{\tau} F(V(Z^l + \tau \delta Z)).$$

To obtain a method similar to the iterative barrier method of Charakhchyan, Ivanenko, 1988 [5], one should set

$$H_{ij} = 0 \quad \text{for } i \neq j. \tag{34}$$

We refer to this method as explicit one since it does not require solver for the solution of the linear system on each iteration. In order to obtain an implicit method similar to the method from [31] one should neglect the nondiagonal elements in the matrices $L_i^T H_{ij} L_j$. As a result, the linear system (32) is split into three independent linear systems with respect to the vectors δz_m , defined by

$$(\delta z_m)_i = (\delta z_i)_m.$$

The resulting linear systems with symmetric positive definite matrices can be solved approximately using the preconditioned conjugate gradient technique. Let us note that the gradient projection technique is a standard tool in the optimization methods and was successfully used in mesh generation, see e.g. [36,46].

The convergence of iterations to a stationary point of the discrete functional was rigorously proven in [33] for the most known polyconvex stored energies and for a quasi-isometric functional.

5. Mesh untangling technique

The variational method can also be used in the case when the algebraic volume of some tetrahedra in an initial mesh is zero or negative. An iterative method in this case is formulated as follows [21]:

$$H^l \delta Z = R^l, \quad \text{where } (\delta R_m^l)_k = (r_k^l)_m, \quad r_k^l = L_k \frac{\partial \Phi_\varepsilon^l}{\partial z_k} \tag{35}$$

$$\varepsilon(Z) = (\delta_0^2 + 0.004 * (\min(0, \min(\det C(Z)_{|i|})))^2)^{\frac{1}{2}}, \quad C = Q \nabla_\xi \chi P^{-1} \tag{35}$$

$$Z^{l+1} = V(Z^l - \tau_l \delta Z) \quad \text{where} \tag{36}$$

$$\tau_l = \arg \min_{\tau} \Phi_\varepsilon(V(Z^l + \tau \delta Z)). \tag{37}$$

Here function $\Phi_\varepsilon : \mathbb{R}^{3 \times n_v} \rightarrow \mathbb{R}$ denotes the discretized penalty functional (15). Formula (35) means that the minimum of the determinant of matrix C is computed over all quadratures nodes of all elements of the mesh Z^l . Parameter δ_0 is certain small positive constant, say $\delta_0 = 10^{-11}$. Since potential P_ε for penalty functional Φ_ε is not polyconvex, generally one cannot guarantee that diagonal blocks of the Hessian matrix of $\Phi_\varepsilon(Z)$ are positive definite. However one can easily prove required positive definiteness provided that terms depending on second derivatives of the function χ are eliminated.

As one can see, steps of the untangling algorithm are quite similar to those for optimization. Moreover, when $\det C$ is positive everywhere they essentially coincide. Careful look at the choice of penalty formulation suggests that during the iterative process elements may travel back and forth from the admissible set. Numerical experiments with block structured grids, presented in the next section, are based on such an approach. Sometimes it is desirable to make element evolution one-way: they may travel into the admissible set but not allowed to get outside. Simple modification of the above scheme

serves to this purpose. When parameter ε is computed using formula (35), it is formally replaced by the value δ_0 for all nondegenerate elements. Hence 1D line search step (37) prevents degeneration of these elements.

Numerical experience shows that sequence of parameters ε^l tends to zero and mesh is untangled and simultaneously optimized in the already untangled subdomains. In [21] it was proven that one can construct the trajectory of the continuation technique with respect to parameter ε such that the solution converges to the stationary point of the functional Φ_{δ_0} .

When admissible mesh is constructed it is usually not far from the optimal solution. Note that algorithms for simultaneous untangling and optimization were also presented in [26,47].

In 2D the above algorithm was found to be quite robust with respect to the initial guess. We did not encounter practical test cases which were not treatable using the technique suggested in [21].

However, in the 3D case performance of the untangling technique based on a penalty functional is less robust with respect to the stiffness of the problem. If the target shapes for the mesh elements are very anisotropic, as it happens while constructing very thick prismatic layers, the iterative untangling procedure can be very slow.

An approach alternative to the penalty technique is a variant of the barrier untangling algorithm based on expansion of the admissible set with subsequent contraction. The idea is to use function $\Psi_\varepsilon(Z)$ (17) instead of penalty functional $\Phi_\varepsilon(Z)$. Parameter ε is chosen in such a way that

$$\det C(Z) + \varepsilon > 0 \tag{38}$$

for all quadrature nodes of all elements. Formula (35) should be replaced by the following one

$$\varepsilon^{l+1} = \max(\delta_0, \varepsilon^l - \sigma(\varepsilon^l - |\min(\det C, 0)|)), \quad 0 < \sigma < 1. \tag{39}$$

This formula guarantees that $\varepsilon^{l+1} < \varepsilon^l$ and ε^{l+1} satisfies (38) with $Z = Z^l$ providing admissible initial guess for iteration $l + 1$. Here it is suggested $\varepsilon^0 = \frac{3}{2}|\min(\det C, 0)|$.

It was proven in [18] that such an algorithm constructs an admissible mesh using only a finite number of exact minimization steps provided that the solution exists, i.e. for a certain number M we get $\varepsilon^l = 0, l \geq M$. Surprisingly, to the best of our knowledge, this algorithm has never been tested before in practical 3D test cases. In practice, one should extract subdomains containing tangled elements and self-intersections and apply the optimization locally, reducing the size of the active set of mesh elements along with the minimization of parameter ε^l .

One should also note that finite untangling proof can be generalized to the penalty algorithm provided that iterative scheme guarantees essential reduction of functional during each iteration.

One can roughly divide the applications of the variational mesh optimization method into two groups with respect to the choice of the iterative solver. The applications for the preconditioned iterative methods include the global surface flattening with a minimal distortion, the global untangling for complicated domains and similar problems in which the initial guess is quite far from the solution and, due to problem formulation, large distortions are present. The applications, in which explicit methods are preferable include the admissible mesh smoothing and optimization, especially in the case of slip boundary conditions and local untangling when the tangled grid contains a relatively small number of elements.

6. Numerical experiments

We consider several examples, which illustrate the performance and robustness of the proposed methods.

6.1. Untangling and optimization of structured meshes

The first test problem is specially devised to test the robustness of the untangling algorithm. Geometric setting is simple and easily reproducible. Consider the unit cube $C = \{x_i : -\frac{1}{2} \leq x_i \leq \frac{1}{2}, i = 1, 2, 3\}$. One can construct in C uniform Cartesian mesh consisting of $n_1 \times n_2 \times n_3$ cubes. All vertices of this mesh which lie inside smaller cube $C_l = \{x_i : -\frac{1}{2\sqrt{2}} \leq x_i \leq \frac{1}{2\sqrt{2}}, i = 1, 2, 3\}$ are rotated around the x_3 axis by the angle α and fixed. The positions of all remaining internal vertices are found using untangling and subsequent optimization procedure. Initial guess in all cases is uniform Cartesian mesh. Results are presented for mesh with $n_1 = n_2 = n_3 = 32$. For this test case it is not possible to deform initial Cartesian mesh into final one using gradual rotation of inner cube and vertex movement keeping mesh admissible. Evidently in order to construct such a deformation one may reduce the size of the inner cube, gradually rotate and restore initial size of the cube. Variational untangling technique is supposed to solve the same problem in a black box mode. Fig. 1 shows certain subset of initial Cartesian mesh elements and the same subsets for deformed meshes for rotation angles $\pi/8, 3\pi/8, \pi/2, 7\pi/8, \pi$. One should note that cases $\alpha = 7\pi/8, \pi$ are quite difficult. Moreover numerical solutions are not unique which is clear from the loss of symmetry of solutions. Similar results for 2D barrier functional were obtained in [21].

Fig. 2 shows three different coordinate surfaces for these test cases.

Fig. 3 shows deformation of the coordinate surface $i_3 = 16$ passing through the center of the cube. Note that for $\alpha = \pi/8$ this coordinate surface remains flat and retains discrete symmetry, while for large angles symmetry is lost. For $\alpha = 7\pi/8$ deviation of this coordinate surface from plane is very large.

Quantitative behavior of the implicit version of an untangling technique is illustrated in Table 1.

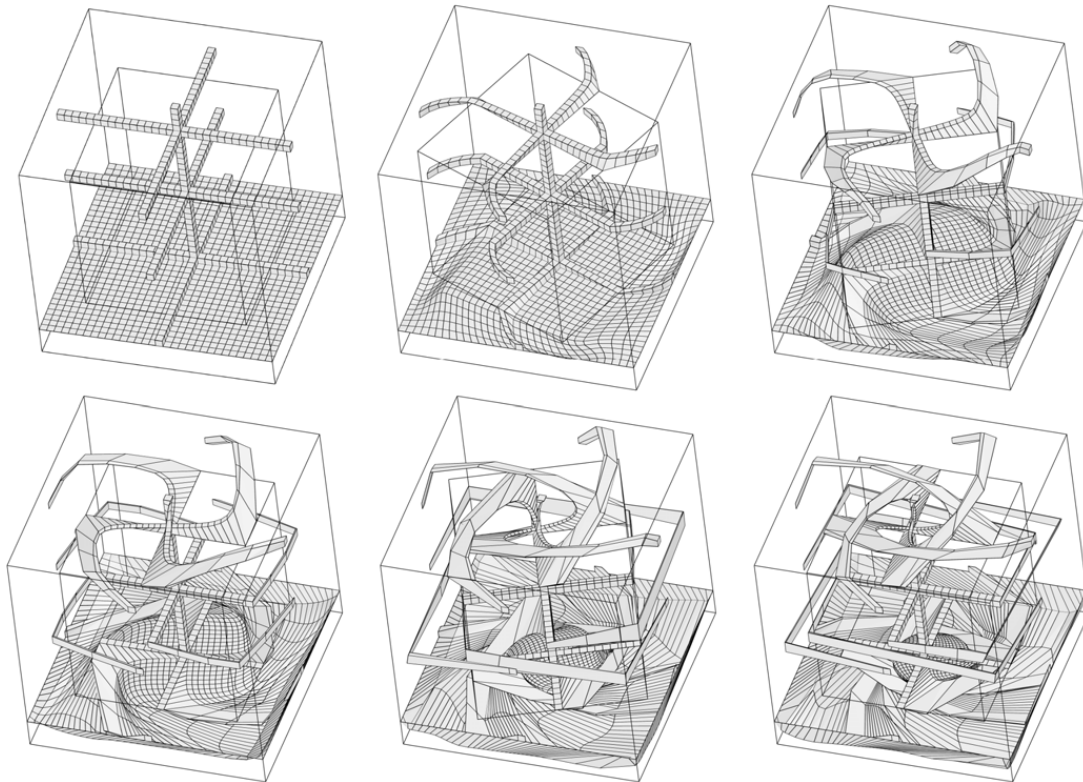


Fig. 1. Rows of elements of resulting mesh and coordinate surface $i_3 = 4$ for $\alpha = 0, \pi/8, 3\pi/8, \pi/2, 7\pi/8, \pi$.

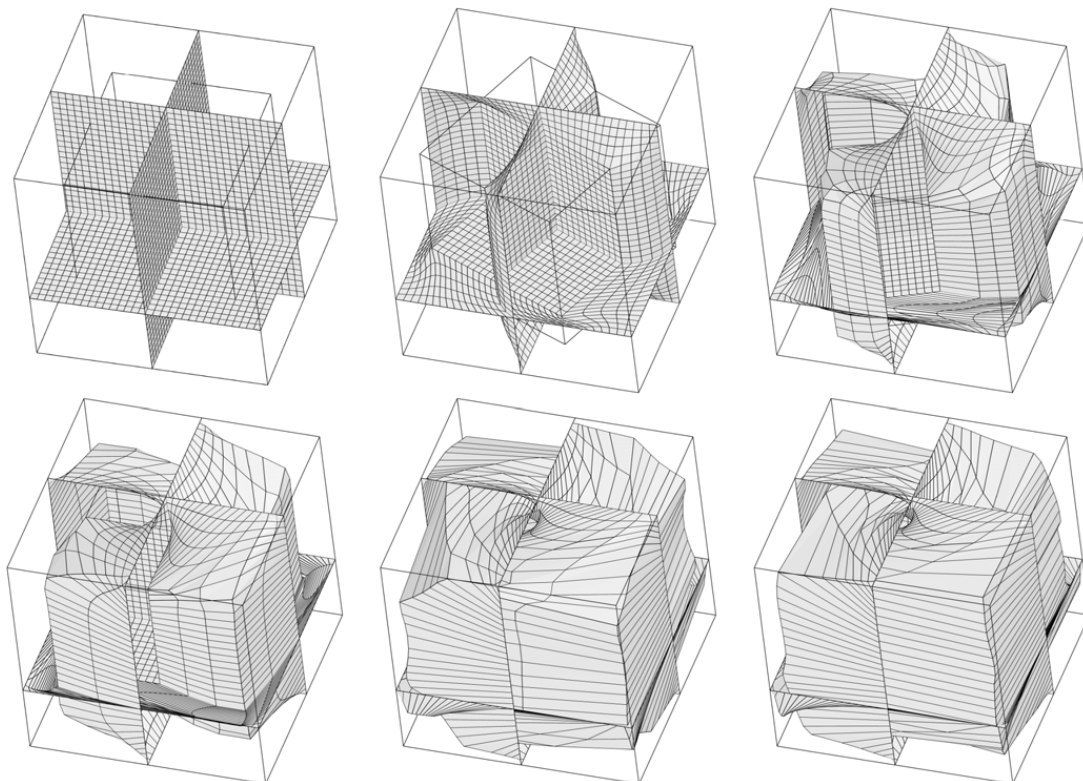


Fig. 2. Three different coordinate surfaces for $\alpha = 0, \pi/8, 3\pi/8, \pi/2, 7\pi/8, \pi$.

Here M_{init} is a number of inverted “tetrahedra” in the initial mesh. “Tetrahedron” here is the geometrical object which generates single contribution to quadrature rule for hexahedral element as explained in (24). Hence corresponding number of degenerate hexahedra is much smaller. M_{max} denotes the maximal number of inverted tetrahedra during the untangling

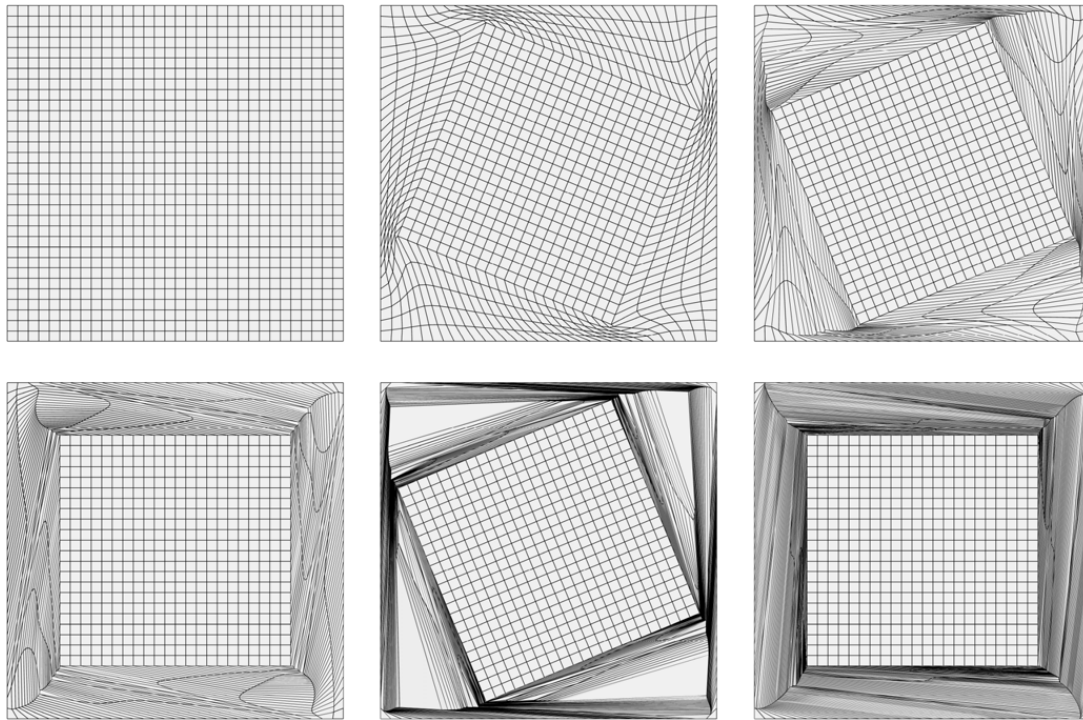


Fig. 3. Coordinate surface $i_3 = 16$ for $\alpha = 0, \pi/8, 3\pi/8, \pi/2, 7\pi/8, \pi$.

Table 1
Untangling results.

α	$\pi/8$	$3\pi/8$	$\pi/2$	$\pi^*/2$	$7\pi/8$	π
M_{init}	19 264	22 400	31 192	124 128	32 032	34 157
M_{max}	19 264	36 029	82 330	663 436	213 554	126 644
$niter$	140	8160	2120	9240	63 600	56 000
t_u	164	8243	2983	67 654	84 562	67 928
ϕ_{min}	4.34×10^{-2}	1.72×10^{-3}	1.97×10^{-3}	7.76×10^{-4}	1.02×10^{-4}	2.65×10^{-4}
ψ_{min}	1.06×10^{-1}	7.0×10^{-3}	1.48×10^{-2}	9.07×10^{-3}	3.05×10^{-4}	1.87×10^{-3}

procedure. Parameter $niter$ denotes the number of untangling iterations sufficient to reach the mesh with total number of inverted tetrahedra less than 100. At that phase fragment containing these tetrahedra is untangled locally without much influence on total wall-clock time. t_u is the CPU time for making $niter$ steps. Timings were obtained on single core of Intel I7 2200HGz. Here ϕ_{min} is the minimal value of the shape quality function $\det C / (\frac{1}{3} \text{tr} C^T C)^{\frac{3}{2}}$ and ψ_{min} is the minimal value of the volumetric quality function $2 \det C / (1 + \det C^2)$, C is the Jacobian matrix. Variant marked with \star corresponds to $64 \times 64 \times 64$ mesh. Figs. 4 and 5 below illustrate comparative behavior of implicit and explicit untangling algorithms.

Obviously, the implicit method is quite efficient but it may spontaneously create localized zones where mesh is knotted which can be attributed to the fact that some descent directions in the implicit method are quite bad. An explicit method generally is knot-free, but the untangling process in general is much slower. This difference is much more pronounced on finer meshes. Note that each iteration of the explicit method is about two times faster compared to the implicit one. For this test case target mesh is uniform. For highly stretched meshes an implicit method is more efficient. Testing the admissible set reduction scheme (17) on the same data sets using parameter sequence (39) leads to the following conclusions: (a) restarts make the untangling algorithm more efficient; (b) for relatively simple test problems, say when $\alpha = \pi/8$, the admissible set reduction algorithm is quite efficient; (c) for stiff problems this algorithm is much slower. One can conclude that the penalty technique is suitable for industrial applications while the admissible set reduction technique is still of theoretical interest.

The second example is related to the construction of structured meshes in complicated domains. Consider a winged body shown in Fig. 6. A geometrical model of the body is given by the surface tessellation that is essentially a triangulation in which the exact surface is approximated with a prescribed chordal error. This triangulation can contain surface triangles with an arbitrarily bad shape.

The surface-curvature sensitive structured surface mesh for this model is constructed using 2D functional (20).

A structured 3D mesh around a winged body is computed using the minimization procedure for the 3D functional 13. To this end, an initial algebraic mesh is constructed. A metric in the Lagrangian coordinates defining the near-wall stretching is prescribed. An implicit iterative minimization solver is used.

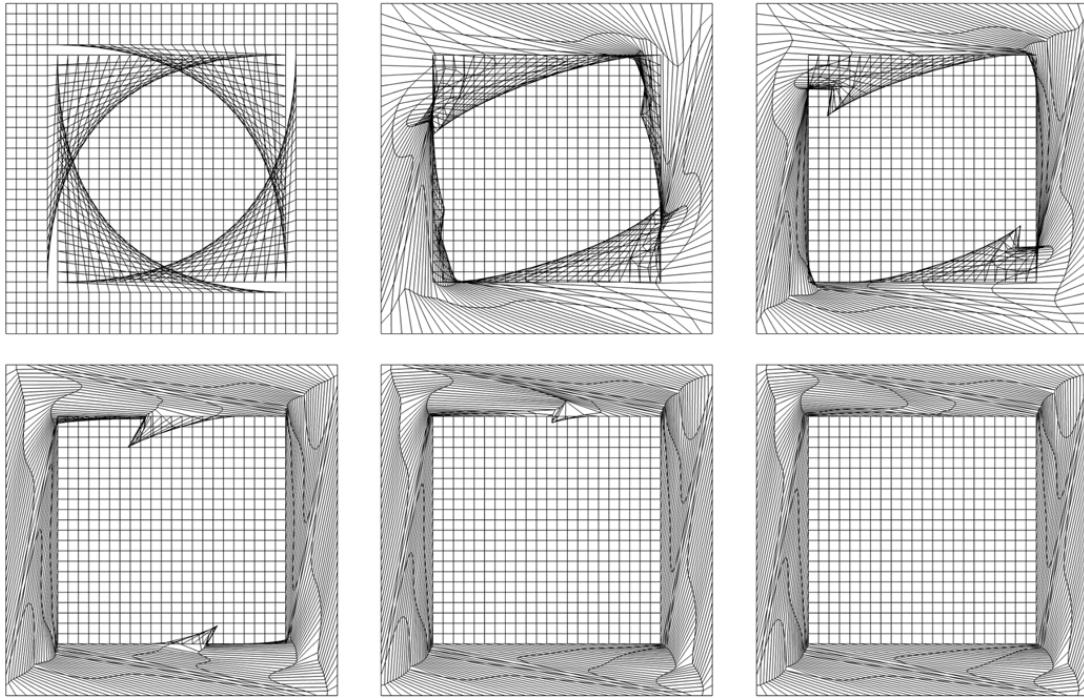


Fig. 4. Implicit method, coordinate surface $i_3 = 16$ for iterations 0, 200, 400, 800, 1200, 1400.

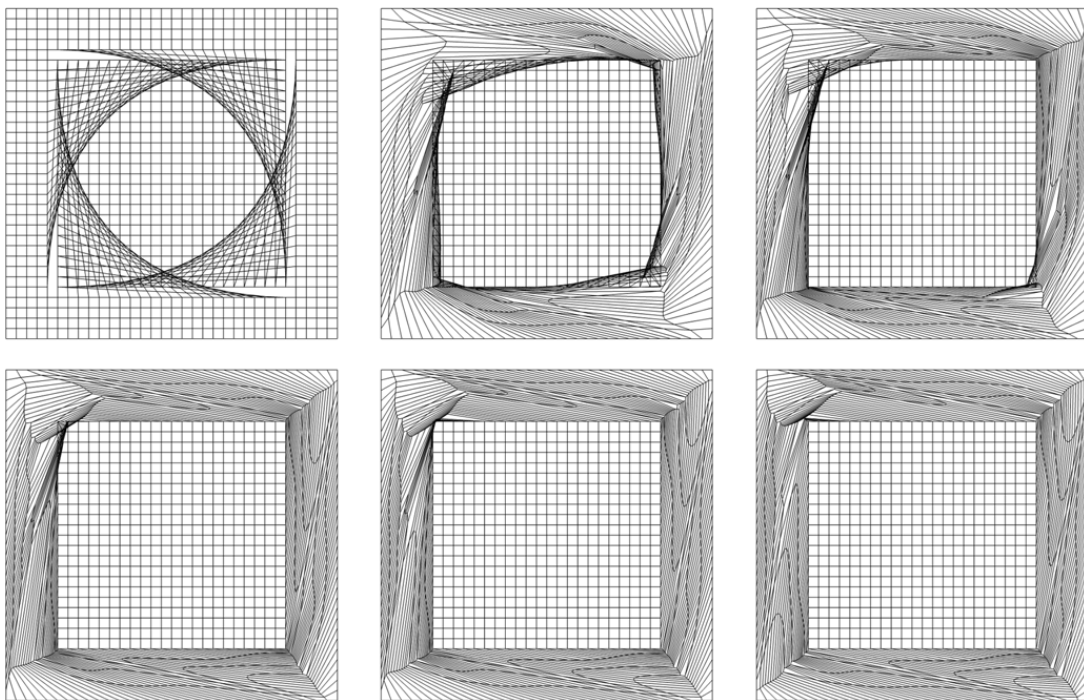


Fig. 5. Explicit method, coordinate surface $i_3 = 16$ for iterations 0, 1600, 3200, 4800, 6400, 7080.

Intermediate untangling results are shown in Fig. 7. For this test case it takes 50 iterations for untangling. The last figure in the series corresponds to the optimized mesh. As one can see, the resulting mesh precisely corresponds to the prescribed near-wall stretching law and the deviation from orthogonality near the surface is negligible.

The global view of the 3D mesh is illustrated in Fig. 8 where three families of coordinate surfaces are presented.

A relatively difficult test problem for the surface and volume meshing algorithm is a swept wing body configuration. The result of the application of the same mesh generation procedure is illustrated in Fig. 9. Here, several coordinate surfaces of 3D mesh are shown including one that corresponds to the surface of the swept wing body. One can see that the mesh stretching is very well controlled and orthogonalization errors near the surface are still negligibly small.

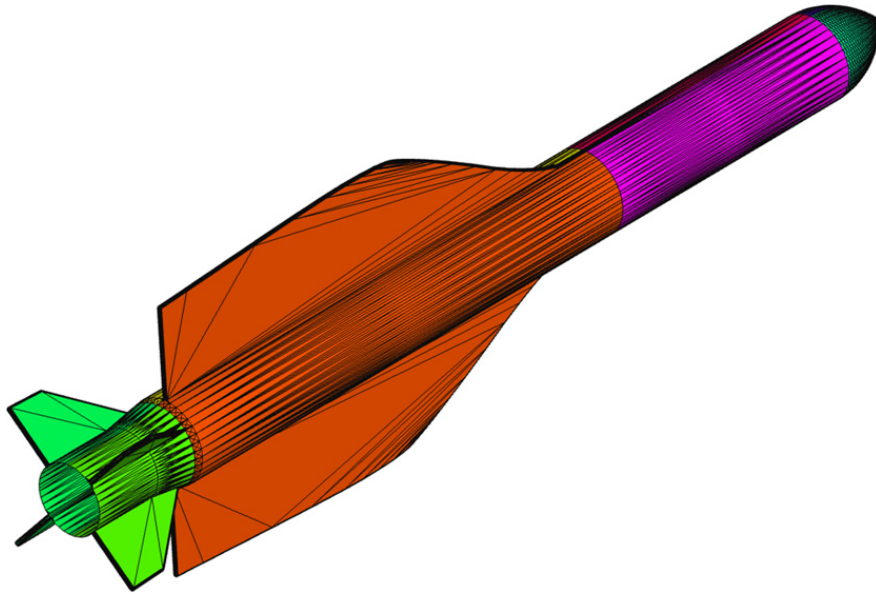


Fig. 6. Tessellated model.

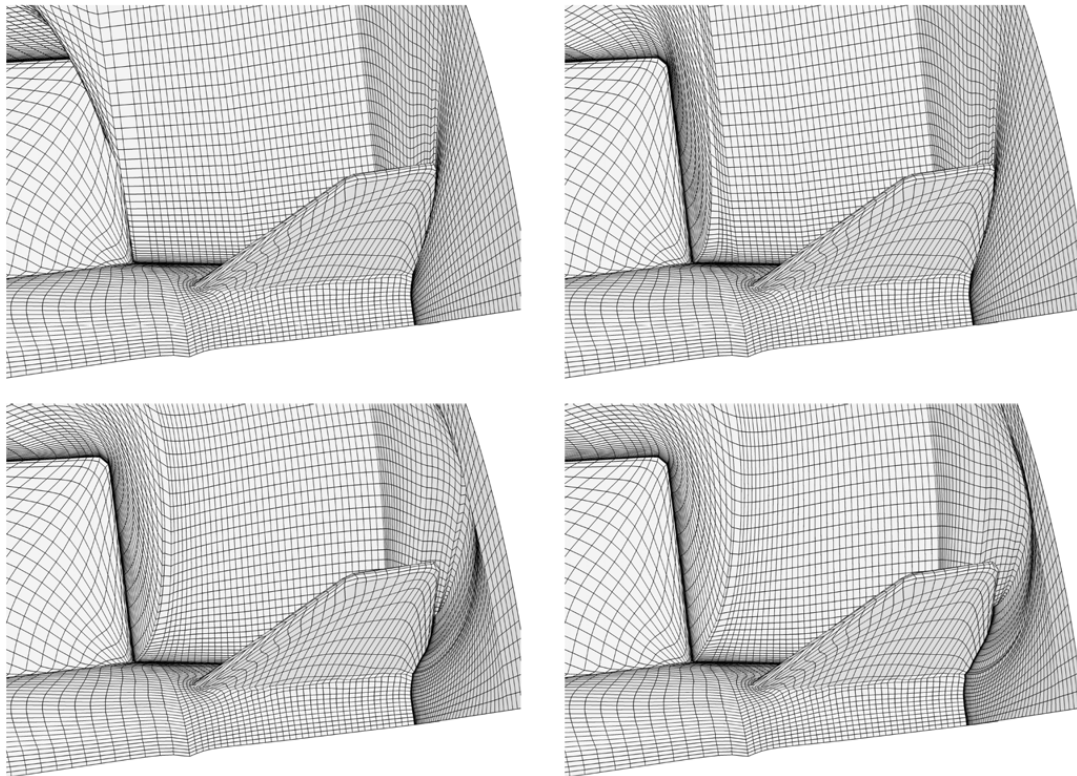


Fig. 7. Successive stages of the untangling procedure.

To alleviate the influence of mesh elements flow over sharp edges on the body, a surface curvature sensitive surface mesh is constructed.

The left-hand side in Fig. 10 shows the example of a surface mesh sensitive to the discrete mean curvature of the surface, while the distribution of the discrete mean curvature on an adaptive mesh being shown on the right-hand side.

As can be expected, the discrete mean curvature field based on the surface tessellation is noisy. A simple filtering technique is applied to alleviate the influence of this noise. When discrete absolute mean curvature is below certain problem dependent threshold it is set to zero, while the values above another positive constant are replaced by this constant.

The next figure illustrates the construction of a surface curvature sensitive 3D mesh as compared to a uniform 3D mesh Fig. 11.

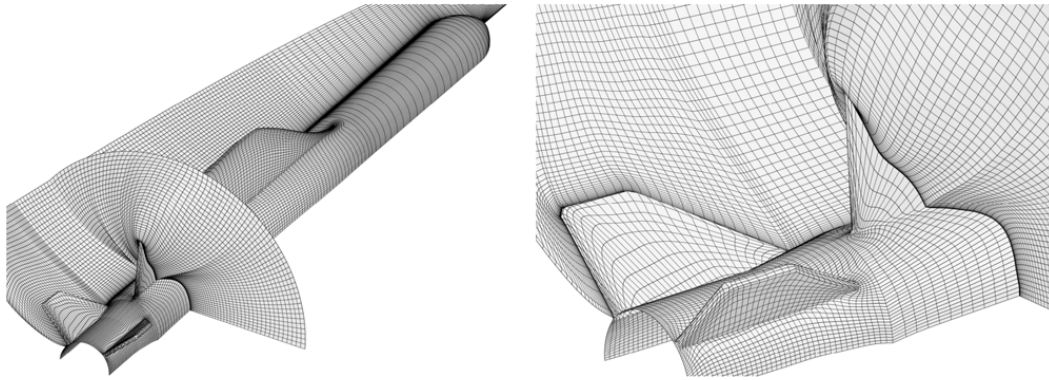


Fig. 8. Coordinate surfaces of 3D mesh around winged body.

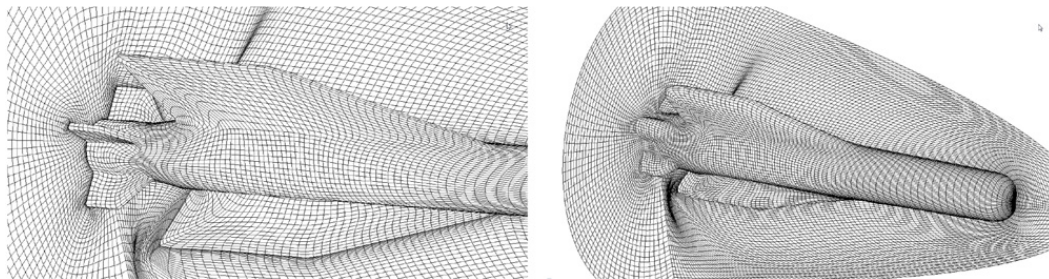


Fig. 9. Coordinate surfaces of 3D mesh for a swept wing configuration.

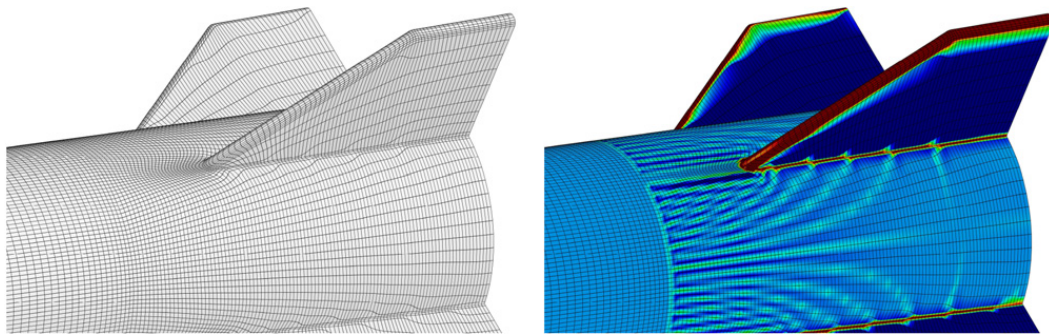


Fig. 10. Curvature sensitive mesh and discrete mean curvature field.

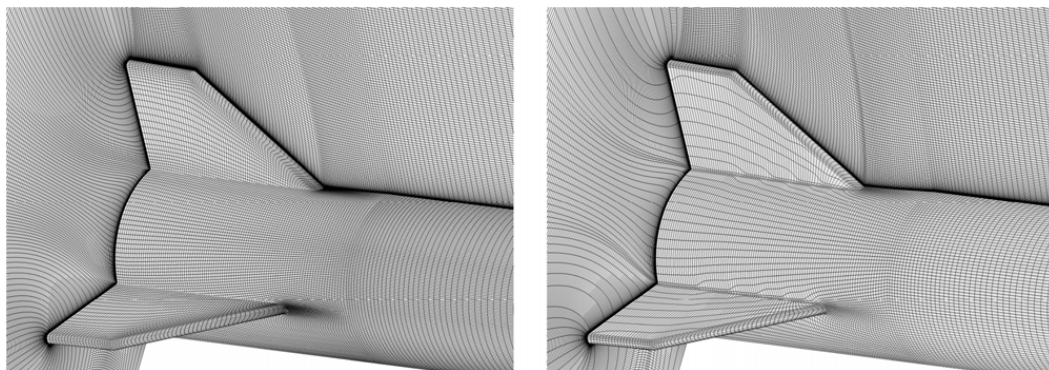


Fig. 11. Left—uniform mesh, right—mean curvature sensitive surface mesh and 3D mesh.

6.2. Construction of large offsets and thick prismatic layers using the variational method

The second application of the suggested variational method is related to the construction of large offsets and thick prismatic mesh layers around complicated bodies. A layer is called “thick” since its thickness is allowed to be comparable to the characteristic size of the geometric model.

Construction of prismatic layer for relatively realistic airplane test model is illustrated in Figs. 12–13.

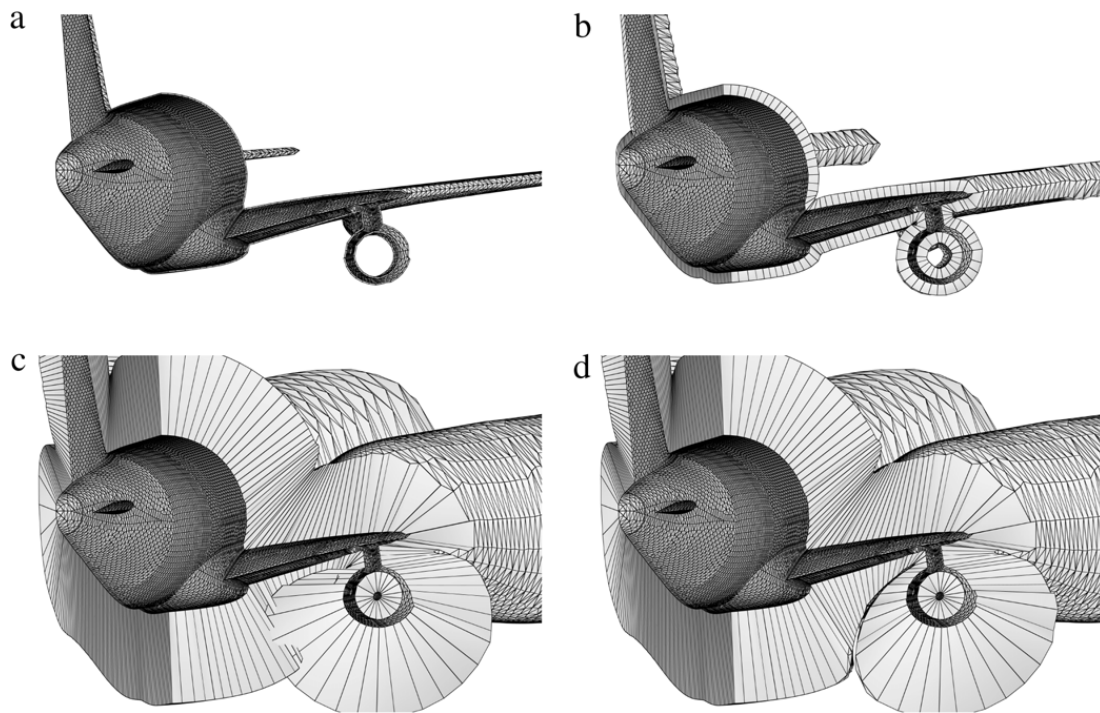


Fig. 12. (a) Initial thin layer, (b) intermediate layer, (c) thick layer, (d) layer with eliminated self-intersections.

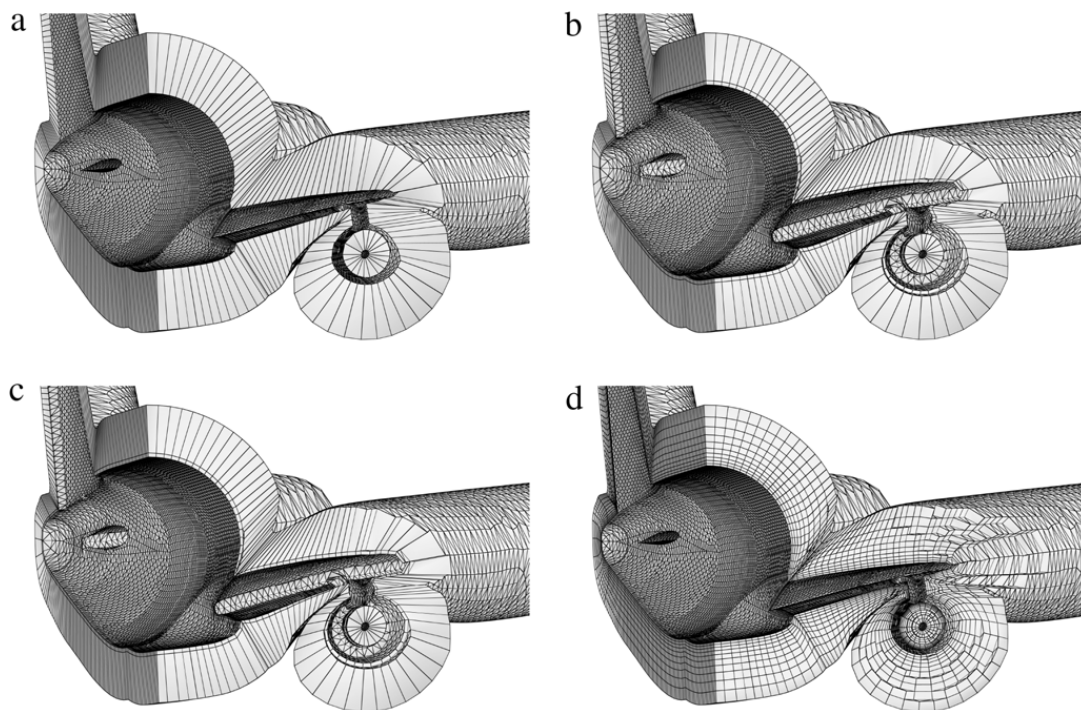


Fig. 13. (a) Layer after the Laplacian–Beltrami smoothing, (b) splitting of current layer into two, (c) orthogonalization of internal layer, (d) final multilayered mesh.

As the first step, one-element-wide prismatic layer of prescribed thickness is constructed. To this end, one first constructs a relatively thin layer using the mesh vertex normals to define the side edges of the prisms as shown in Fig. 12(a). The maximal thickness of this layer is bounded from above by the prism nongeneracy condition. Each prism is assumed to consist of an elastic material which is highly compressed in the direction normal to the surface in Lagrangian coordinates. Hence, one can solve stationary elastic springback problem by minimizing functional (13) and prescribing for each prism in the layer a target shape with a certain height (thickness). An intermediate solution to the springback problem is shown in Fig. 12(b). The result of untangling and optimization is a relatively thick layer which does not contain degenerate prisms. However, it may contain overlaps and self-intersections as shown in Fig. 12(c).

To eliminate self-intersections, a special iterative procedure for cutting excessive material is applied. If an intersection between prisms is detected, then the height of both prisms is reduced by a certain value chosen to be quite close to unity. Successive application of this procedure reduces the number of self-intersections and eventually eliminates them creating an approximate contact spot, which resembles a medial surface. The result of such a procedure is illustrated in Fig. 13(a).

Additional material is eliminated to restore precise layer thickness. This process is coupled with the Laplace–Beltrami smoothing of final offset surface. Discrete approximation of the Laplace–Beltrami operator is constructed using the mean value theorem for harmonic functions [35]. In the process of smoothing only vertex movement along outgoing edges of prismatic mesh is allowed. The result is shown in Fig. 13(a).

To construct the final multilayered prismatic mesh, a combination of the marching technique and the variational method is applied. At each step a one-layered mesh is split into two sublayers, and the variational optimization is applied to the resulting prismatic mesh which tends to orthogonalize the inner layer. Fig. 13(b)–(c) illustrate this step as applied to the final mesh layer number four. After few optimization iterations the inner layer is extracted and added to the pool of the computed layers. The same algorithm is again applied to the remaining one-layered mesh. This procedure is repeated until the initial layer is exhausted. Optionally, in order to prevent mesh element skewing, near-external-boundary subdivision/optimization steps can be stopped before the exhaustion of initial layer and the remaining layer containing skewed elements can be just thrown away.

The above procedure is rather complicated. However, it guarantees that at each step of construction prismatic mesh elements remain nondegenerate, even though the deformations can be quite large. This property is crucial for really thick layers where very long prisms with a small base can appear. It has to be noted that simple marching algorithms can very easily lead to degeneration of such elements.

One should also note that for the elastic springback phase an implicit iterative solver is used, since an explicit solver is not powerful enough to converge and reach the target thickness of the layer. Meanwhile, the optimization for marching generation of layers is based on a less expensive explicit minimization iterative solver.

One can easily see that deviation from orthogonality near the boundary is negligible and the overall quality of the prismatic layer makes it useful for industrial flow simulations. The resulting algorithm is integrated into pre- and postprocessor of multiphysics simulation code LOGOS [48].

7. Conclusions

Theoretical foundations for variational mesh optimization methods have been presented. We have introduced a variational method which can provably construct 3D quasi-isometric mappings between domains of a complex shape. A local maximum principle for polyconvex distorted measures has been formulated which allows us to control the invertibility and distortion bounds for non-simplicial elements in the process of minimization. The simple and efficient technique for construction of boundary orthogonal meshes suggested in [31] has been applied to the construction of hexahedral meshes and thick prismatic mesh layers around complex shapes. The untangling technique which is a generalization of the method proposed in [21] has been verified on a wide set of challengeable test problems. Another untangling technique based on [49], which provably constructs admissible meshes using finite number of minimization steps, has been implemented.

A minimization technique for the mesh functional has been formulated. The approach is based on the global gradient descent technique with preconditioning using domain decomposition for local mesh optimization and untangling. Slip boundary conditions for implicit domains are incorporated into the iterative minimization procedure.

It is shown that implicit solver is well suited for global surface flattening with minimal distortion, global untangling for complicated domains, optimization of meshes and mappings for stiff problem. The main advantages of this technique are stability and robustness. An explicit method is better suited for mesh smoothing and optimization, especially in the case of slip boundary conditions and local untangling. This technique is considerably faster per iteration. However, we were not able to solve certain problems using explicit solver.

For further reading

[50], [51] and [52].

Acknowledgments

This work has been supported by the Russian government under grant Measures to Attract Leading Scientists to Russian Educational Institutions (contract No. 11.G34.31.0072). Partial support of Presidium RAS grant P-18 and RFBR grant 14-07-00805 is gratefully acknowledged.

References

- [1] W.P. Crowley, An Equipotential Zoner on a Quadrilateral Mesh, Memo, Lawrence Livermore National Lab, 1962.
- [2] A.M. Winslow, Numerical solution of the quasilinear Poisson equation in a nonuniform triangle mesh, *J. Comput. Phys.* 2 (1967) 149–172.
- [3] J.U. Brackbill, J.S. Saltzman, Adaptive zoning for singular problems in two dimensions, *J. Comput. Phys.* 46 (1982) 342–368.

- [4] O-P. Jacquotte, A mechanical model for a new mesh generation method in computational fluid dynamics, *Comput. Methods Appl. Mech. Engrg.* 66 (1988) 323–338.
- [5] S.A. Ivanenko, Construction of nondegenerate grids, *Comput. Math. Math. Phys.* 28 (5) (1988) 141–146.
- [6] V.D. Liseikin, On the construction of regular grids on n -dimensional surfaces, *Comput. Math. Math. Phys.* 31 (11) (1991) 47–57.
- [7] V.D. Liseikin, *Grid Generation Methods*, Springer, Berlin, Heidelberg, New York, 1999.
- [8] P.M. Knupp, Achieving finite element mesh quality via optimization of the Jacobian matrix norm and associated quantities. Part I: a framework for surface mesh optimization, *Int. J. Numer. Methods Eng.* 48 (3) (2000) 401–420.
- [9] P.M. Knupp, Achieving finite element mesh quality via optimization of the Jacobian matrix norm and associated quantities. Part II: a framework for volume mesh optimization and the condition number of the Jacobian matrix, *Int. J. Numer. Methods Eng.* 48 (8) (2000) 1165–1185.
- [10] P. Knupp, Algebraic mesh quality metrics, *SIAM J. Sci. Comput.* 23 (2001) 193–218.
- [11] P.M. Knupp, A method for hexahedral mesh shape optimization, *Int. J. Numer. Methods Eng.* 58 (2) (2003) 319–332.
- [12] L.A. Freitag, P.M. Knupp, Tetrahedral mesh improvement via optimization of the element condition number, *Int. J. Numer. Methods Eng.* 53 (2002) 1377–1391.
- [13] V.D. Liseikin, *Grid Generation Methods*, second ed., Springer-Verlag, Berlin, Heidelberg, New York, 2010.
- [14] J.F. Thompson, B.K. Soni, N. Weatherill (Eds.), *Handbook of Grid Generation*, CRC Press, 1998.
- [15] M.F. Beg, M.I. Miller, A. Trounev, L. Younes, Computing large deformation metric mappings via geodesics flows of diffeomorphisms, *Int. J. Comput. Vis.* 61 (2) (2005) 139–157.
- [16] A. Trounev, An Approach of Pattern Recognition through Infinite Dimensional Group Action, Research Report LMENS-95-9, 1995.
- [17] M. Rumpf, A variational approach to optimal meshes, *Numer. Math.* 72 (4) (1996) 523–540.
- [18] S.A. Ivanenko, Adaptive-harmonic grids. Preprint, Computing Center RAS, 1997.
- [19] K. Rienslagh, J. Vierendeels, Grid generation for complex shaped moving domains, in: Proc. of the 5th Int. Conf. on Numerical Grid Generation in CFD and related Fields, Starkville, Mississippi, April 1996, pp. 569–578. Mississippi State University, 1996.
- [20] K. Rienslagh, J. Vierendeels, E. Dick, Two-dimensional incompressible Navier–Stokes calculations in complex-shaped moving domains. A celebration of the sixty-fifth anniversary of Pieter J. Zandbergen: teacher and research leader in applied mathematics, *J. Engrg. Math.* 34 (1–2) (1998) 57–73.
- [21] V.A. Garanzha, I.E. Kaporin, Regularization of the barrier variational method for constructing computational grids, *Comput. Math. Math. Phys.* 39 (9) (1999) 1426–1440.
- [22] L.A. Freitag, P. Plassmann, Local optimization-based simplicial mesh untangling and improvement, *Int. J. Numer. Methods Eng.* 49 (1–2) (2000) 109–125.
- [23] P.M. Knupp, Hexahedral and tetrahedral mesh untangling, *Eng. Comput.* 17 (2001) :261–268.
- [24] V.A. Garanzha, Maximum norm optimization of quasi-isometric mappings, *Numer. Linear Algebra Appl.* 9 (6–7) (2002) 493–510.
- [25] L.V. Brantets, V.A. Garanzha, Distortion measure for trilinear mapping. Application to 3-D grid generation, *Numer. Linear Algebra Appl.* 9 (6–7) (2002) 511–526.
- [26] J.M. Escobar, E. Rodriguez, R. Montenegro, G. Montero, J.M. Gonzalez-Yuste, Simultaneous untangling and smoothing of tetrahedral meshes, *Comput. Methods Appl. Mech. Eng.* 192 (2003) 2775–2787.
- [27] P. Vachal, R.V. Garimella, M.J. Shashkov, Untangling of 2D meshes in ALE simulations, *J. Comput. Phys.* 196 (2) (2004) 627–644.
- [28] E.J. Lopez, N.M. Nigro, M.A. Storti, Simultaneous untangling and smoothing of moving grids, *Int. J. Numer. Methods Eng.* 76 (7) (2008) 994–1019.
- [29] J. Danczyk, K. Surech, Finite element analysis over tangled simplicial meshes: theory and implementation, *Finite Elem. Anal. Des.* 70–71 (2013) 57–67.
- [30] S.K. Godunov, V.M. Gordienko, G.A. Chumakov, Quasi-isometric parametrization of a curvilinear quadrangle and a metric of constant curvature, *Siberian Adv. Math.* 5 (2) (1995) 1–20.
- [31] V.A. Garanzha, The barrier method for constructing quasi-isometric grids, *Comput. Math. Math. Phys.* 40 (11) (2000) 1617–1637.
- [32] V.A. Garanzha, Quasi-isometric surface parameterization, *Appl. Numer. Math.* 55 (3) (2005) 295–311.
- [33] V.A. Garanzha, I.E. Kaporin, On the convergence of a gradient method for the minimization of functionals in the theory of elasticity with finite deformations and for the minimization of barrier grid functionals, *Comput. Math. Math. Phys.* 45 (8) (2005) 1400–1415.
- [34] V.A. Garanzha, Polyconvex potentials, invertible deformations and thermodynamically consistent formulation of nonlinear elasticity equations, *Comp. Math. Math. Phys.* 50 (9) (2010) 1561–1587.
- [35] M.S. Floater, K. Hormann, Surface parameterization: a tutorial and survey. advances in multiresolution for geometric modelling, *Math. Vis.* (2005) 157–186.
- [36] O.-P. Jacquotte, Grid optimization methods for quality improvement and adaptation, in: J.F. Thompson, B.K. Soni, N. Weatherill (Eds.), *Handbook of Grid Generation*, CRC Press, 1998, Section 33.
- [37] S.M. Shontz, S.A. Vavasis, A robust solution procedure for hyperelastic solids with large boundary deformation, *Eng. Comput.* 28 (2) (2012) 135–147.
- [38] J.M. Ball, Convexity conditions and existence theorems in nonlinear elasticity, *Arch. Ration. Mech. Anal.* 63 (1977) 337–403.
- [39] J.M. Ball, Global invertibility of Sobolev functions and the interpenetration of matter, *Proc. Roy. Soc. Edinburgh.* 88A (1981) 315–328.
- [40] A. Liu, B. Joe, On the shape of tetrahedra from bisection, *Math. Comput.* 63 (1994) 141–154.
- [41] S.P. Sastry, S.M. Shontz, S.A. Vavasis, A log-barrier method for mesh quality improvement, in: *Proceedings of the 20th International Meshing Roundtable*, Springer, 2011, pp. 329–346.
- [42] S.P. Sastry, S.M. Shontz, S.A. Vavasis, A log-barrier method for mesh quality improvement and untangling, *Eng. Comput.* (November 2012) Published online ahead of print.
- [43] S.A. Ivanenko, Grid generation with cell shape control, *Comp. Math. Math. Phys.* 40 (11) (2000) 1662–1684.
- [44] S.A. Vavasis, A Bernstein–Bezier Sufficient Condition for Invertibility of Polynomial Mapping Functions, Research Report CoRR cs.NA/0308021, 2003.
- [45] G. Farin, *Curves and Surfaces for Computer-aided Geometric Design*, fourth ed., Academic Press, 1997.
- [46] S.M. Shontz, S.A. Vavasis, A mesh warping algorithm based on weighted Laplacian smoothing, in *Proceedings of the 12th International Meshing Roundtable*, 2003, Santa Fe, NM, pp. 147–158.
- [47] J. Kim, T. Panitanarak, S.M. Shontz, A multiobjective mesh optimization framework for mesh quality improvement and mesh untangling, *Internat. J. Numer. Methods Engrg.* 94 (1) (2013) 20–42.
- [48] A.S. Kozelkov, Yu.N. Deryugin, D.K. Zelensky, V.A. Glazunov, A.A. Golubev, O.V. Denisova, S.V. Lashkin, R.N. Zhuchkov, N.V. Tarasova, M.A. Sizova, Multifunctional package LOGOS for solution of problems of hydrodynamics and heat and mass transfer on supercomputers. Basic technologies and algorithms, in: Abstracts of XIV International Workshop “Supercomputing and Mathematical Modeling”, October 1–5 2012, Sarov, Russia, 215–230 (in Russian).
- [49] A.A. Charakhchyan, S.A. Ivanenko, A variational form of the Winslow grid generator, *J. Comput. Phys.* 136 (1997) 385–398.
- [50] L. Brantets, G.F. Carey, Extension of a mesh quality metric for elements with a curved boundary edge or surface, *J. Comp. Inf. Sci. Eng.* 5 (4) (2005).
- [51] J.M. Ball, Some open problems in elasticity, in: *Geometry, Mechanics, and Dynamics*, Springer, New York, 2002, pp. 3–59.
- [52] S.V. Utyuzhnikov, D.V. Rudenko, An adaptive moving mesh method with application to nonstationary hypersonic flows in the atmosphere, *Proc. Inst. Mech. Eng. G* 222 (5) (2008) 661–671.